Available online at www.sciencedirect.com

ScienceDirect

Procedia Structural Integrity 2 (2016) 2113–2122

Structural Integrity Procedia

www.elsevier.com/locate/procedia

21st European Conference on Fracture, ECF21, 20-24 June 2016, Catania, Italy

Study of the plastic behavior around the crack tip by means of thermal methods

F. Ancona*, R. De Finis, G. P. Demelio, U. Galietti, D. Palumbo

Politecnico di Bari, Department of Mechanics, Mathematics and Management, Viale Japigia 182, 70126, Bari, Italy

Abstract

In this work, the behaviour of two cracked stainless steel AISI 410 and C3FM was studied by means of a new procedure based on thermographic methods. A temperature model in time domain was considered in order to obtain information about the first and the second order harmonic of the temperature signal. Interesting results were obtained in term of possibility to describe the plastic phenomena at the crack tip.

Keywords: Fracture Mechanics; TSA; Crack Growth; Stainless Steels

1. Introduction

The study of the behaviour of cracked materials subjected to dynamic loading implies the knowledge of both the stress intensity factor (SIF) and the crack growth rate (*da/dN*) Paris et al. (1963), Ritchie (1999). In this regard, these parameters can be obtained by use of conventional methods according to Standards (ASTM, 2004), by means of experimental and non-destructive techniques. In particular, the most widely diffused methods used for the monitoring and the measurement of crack growth rate are microscopy, extensometry, ultrasound, X-ray and DIC (Digital Image Correlation), Rèthore et al. (2012).

Saka et al. (1998), proposed a non-destructive method for evaluating a 3D surface crack based on a magnetic field

* Corresponding author. Tel.: +39 3391870405;
E-mail address: francesco.ancona@poliba.it

10.1016/j.prostr.2016.06.265

induced in the air by DC current flow in materials. This method requires two probes for application of the DC current and cracks have to be extremely small in comparison with the distance between the probes. A 3D X-ray synchrotron tomography was used by Williams et al. (2013) to obtain local measurements of crack growth in a 7075-T6 aluminum alloy. This instrumentation allows for in situ measurements of crack opening displacement (COD) but requires a suited precision alignment fixture for *in situ* testing.

In Kainuma's work (2015), a quantitative examination of the efficiency of micro-encapsulated dye mixing paint was performed. This method allows for an easily applicable inspection also on actual structural components while, The magnetic flux density around the fatigue crack was observed in the work of Tanabe et al. (2011). However, these techniques do not allow for an accurate crack length measurement.

Infrared thermography (IRT) was also proposed for the study of the fracture behaviour of materials subjected to fatigue loading, Carrascal et al. (2014), Guduru et al. (2001), Fedorova et al. (2012), Tomlinson et al. (1999), Tomlinson et al. (2011), Diaz et al. (2004), Diaz et al. (2013), Diaz et al. (2005), Ancona et al. (2015), Palumbo et al. (2015). In particular, a temperature rise due to the heat dissipations can be observed around the crack tip where the plastic zone is located. In this regard, Carrascal et al. (2014) used IRT for evaluating the Paris Law constants of a polymer (polyamide) with an experimental methodology. A good agreement was found with respect to traditional calculation methods. However, this procedure may find limitation in those cases in which temperature changes on material related to the plastic zone are very low (short cracks) and, moreover, high performance equipment and a difficult set-up are required. This is the case, for instance, with brittle materials (such as martensitic steels), welded joints and aluminum alloys, Palumbo et al. (2014), Galietti et al. (2010), Galietti et al. (2013), Galietti et al. (2014).

The aim of this work is to propose an innovative procedure to study the dynamic crack behaviour of materials based on the analysis in time domain of the thermal signal.

Thermoelastic Stress Analysis (TSA) technique can be used for the determination of the stress intensity factor during fracture mechanics tests, Dulieu-Barton (1999), Pitarresi et al. (2003), Wang et al. (2010), Harwood et al. (1991), Palumbo et al. (2016). By assessing the sum of the principal stresses, it is possible to determine the stress intensity factor and, at the same time, it is possible to determine the crack growth rate by analyzing the phase data, Diaz et al. (2004). In particular, Tomlinson et al. (2011) demonstrated the potential of TSA by using the amplitude of the thermoelastic signal for the crack tip and the SIF evaluation. In the works of Diaz et al. (2004), Diaz et al. (2005) the phase signal was proposed for detecting the crack tip position. In literature, phase signal is also considered as an effective parameter for the identification of local damage and for the evaluation of fatigue damage in materials, Palumbo et al. (2014), Galietti et al. (2010), Galietti et al. (2013), Galietti et al. (2014).

CT steels specimens were used and tested according to ASTM E 647-00 for the monitoring of crack tip growth in a continuous manner by means of a cooled IR camera. Two stainless steels were tested, AISI 410 with martensitic lattice and CF3M with austenite lattice. These steels are used in engineering fields where resistance to high temperatures, corrosive environments and high mechanical stress are required, McGuire (2008), Tomei (1981). However, despite their wide use in engineering, there is for these materials, no data are available in literature about their fatigue and fracture behaviour. The analysis of thermographic data allows for obtaining the crack tip and the plastic areas. Finally a comparison between the behaviour of the two steels was performed.

2. Experimental set-up

2.1. Specimen geometry and materials

Two stainless steels were used in this work, AISI 410 with martensitic lattice and CF3M with austenitic lattice. Martensitic stainless steels have a higher mechanical strength obtained by a quenching heat treatment compared with austenitic steels; the corrosion resistance is higher in austenitic stainless steel due to the higher percentage of chromium. In Tables 1 the mechanical properties of the stainless steel tested in this work are presented, Tomei (1981).

Three Compact Tension (CT) specimens were used with dimensions according to ASTM E 647 for each material tested. In Figure 1, dimensions of the specimen are reported in mm. Specimens were sprayed with flat black spray to increase the emissivity to 0.95.

Table 1: Mechanical properties (at room temperature) of stainless steels tested in the work

Materials	**E** [MPa]	σ_y[MPa]	σ_{UTS}[MPa]
AISI 410	200,000	639	850
CF3M	200,000	276	586

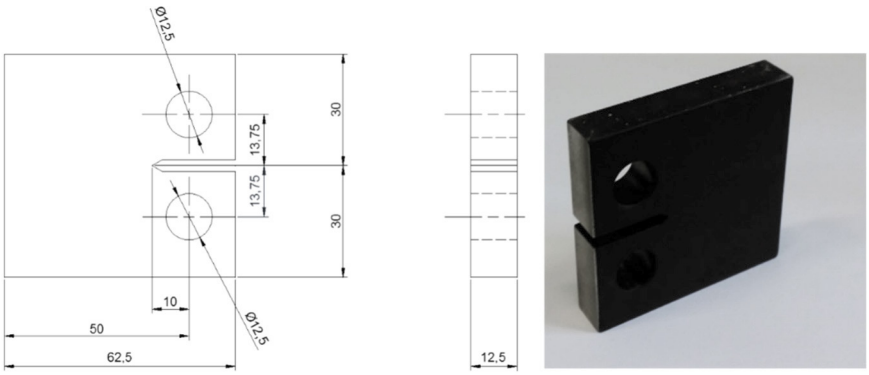

Fig. 1. Specimen dimension in mm according to ASTM E 647-00.

2.2. Testing procedure

The tests were carried out with the MTS model 370 servo hydraulic fatigue machine with a 100 kN capacity. According to ASTM E 647 the constant-force-amplitude procedure was used with a constant force range ΔP, fixed stress ratio ($R=0.1$) and loading frequency f=13 Hz. In Table 3, the loading ranges used during the tests for each material are reported.

Table 2: Loading amplitude used for the materials.

Material	**ΔP** [kN]
AISI 410	10.8
CF3M	9.90

Three thermographic sequences were acquired at intervals of 4000, 48000 and 112000 cycles by using a cooled FLIR IR X6540 SC infrared camera with an InSb detector (640x512 pixels) and acquisition rate of 123 Hz, Figure 2. A geometrical resolution of 0.067 mm/pixel was obtained by placing the thermocamera at 170 mm from the specimen and by using a 50 mm lens with a 12 mm extension ring. All specimens were pre-cracked to a crack length of 2.5 mm according to ASTM E-647.

A second infrared camera, Deltatherm 1560 by Stress Photonics, with an InSb photonic detector (320x256 pixels) on the opposite side of the specimen was used only to monitor the crack size according to Standard.

Fig. 2. Experimental set-up used for testing.

3. Methods and data analysis

Generally, during fatigue tests, two thermal effects related to elasto-plastic properties and mechanical hysteresis are generated. In this way, two heat sources responsible for temperature variations within the specimen can be considered: thermomechanical couplings and intrinsic dissipation, Rosner et al. (2001), Chrysochoos et al. (2009). The first represents the well-known thermoelastic coupling and all the other thermomechanical couplings associated with interactions between the temperature and microstructure while, intrinsic dissipation is thermodynamically irreversible and is due to micro-plastifications and anelastic effects, Rosner et al. (2001), Chrysochoos et al. (2009).

Under the hypotheses of absence of thermomechanical couplings due to microstructure in material in a homogeneous Hookean material under adiabatic conditions, the temperature changes ΔTel due to thermomechanical couplings are due only to thermoelastic sources, Dulieu-Barton (1999), Pitarresi et al. (2003), Wang et al. (2010), Harwood et al. (1991), Palumbo et al. (2016). Temperature variation over time can be described in the case of uniaxial stress with sinusoidal loading:

$$T_{el} = KT_0\sigma_a \sin(\omega t + \pi + \varphi) \tag{1}$$

where $K = \alpha/(\rho Cp)$ is the thermoelastic constant, T_0 is the absolute temperature, σ_a is the stress semi-amplitude and φ is the phase angle between temperature and loading signal. This angle remains constant in presence of linear elastic behaviour of material and it changes:

1. in presence of viscoelastic or plastic behaviour of material, Pitarresi et al. (2003), Connesson et al. (2011).
2. in presence of high stress gradient leading to heat conduction in material and to the loss of adiabatic conditions, Pitarresi et al. (2003), Wang et al. (2010).

In particular, during a fatigue test, the phase signal remains constant up to the occurrence of plastic behaviour in the material and with increasing of damage, phase variations can be observed due to the previously discussed phenomena either in negative and positive values, Palumbo et al. (2014), Galietti et al. (2010), Galietti et al. (2013), Galietti et al. (2014).

Temperature variations T_{diss} due to intrinsic dissipation represent the largest components of the Fourier sine series that occurs at twice the frequency of mechanical loading and elastic response T_{el}. Indeed, for each cycle of elastic temperature response, two cycles of plastic temperature response occur. Different works used this Fourier component (at twice the mechanical frequency) to characterize the fatigue damage of material, Enke et al. (1988), Sakagami et al. (2005) and to estimate the fatigue limit, Krapez et al. (2000).

In order to investigate the just described temperature signal components, a mathematical algorithm has been used to extract pixel by pixel phase angle and the amplitude of the first and second Fourier harmonic components. In particular, a suited temperature model has been used to study the thermal signal Tm in the time domain, as indicate in equation (1):

$$T_m(t) = a + bt + T1\sin(\omega t + \varphi 1) + T2\sin(2\omega t + \varphi 2) \tag{2}$$

where the term a + bt represents the increase in mean temperature during the cyclic mechanical loading, ω is angular frequency of the mechanical imposed load, T1 and φ1 are respectively amplitude and phase of first harmonic component of Fourier series of the thermographic signal while, T2 and φ2 represent the amplitude of the second Fourier harmonic component. By considering equation 1, the term T1 corresponds to the temperature variation related to thermoelastic effect, while T2 term is proportional to the amplitude of intrinsic dissipation.

Equation (2) is integrated in the algorithm of software IRTA® providing image in form of data matrix for each constant parameter.

4. Results

As exposed in the previous section, the proposed algorithm leads to assess 5 different parameters from each thermographic sequence: a, T1, T2, φ1 and φ2. In figure 3 are shown the temperature maps (a) for the two materials obtained in correspondence of the same value of SIF (K_I=23.6 MPa $m^{1/2}$) and a crack length of about 4 mm for both materials. It is worth noting to underline that no significant temperature values are measured around the crack tip because of the presence of localized heat sources in a small area of specimen. These results demonstrate that the temperature cannot be used for the monitoring of crack mostly at the early stage of growth.
In figure 4 is shown the map of the second harmonic of thermographic signal (T2) for AISI 410 steel. In particular, two area (A1 and A2) characterized by a significant value of the signal are clearly visible along the crack growth direction. In figure 4 is shown also the signal trend along the considered profile. This particular behaviour is due to two different effects: the contact between the crack faces (A1 area) and the plastic conditions ahead of the crack tip (A2 area). Interesting results were obtained also analyzing the phase signal of 2ω component, figure 5. In this case, a phase signal inversion is obtained by passing from A1 to A2 area.
Similar signal profiles were also obtained for the austenitic steel CF3M. This last is characterized by a more ductile behaviour and an irregular crack growth direction. However, as shown in figures 6 and 7, similar considerations about T2 component and phase signal φ2 can be applied.
Amplitude and phase of 2ω component were compared with the phase of thermoelastic signal generally used for evaluating the plastic area, the crack tip and the "notional" crack tip considering the Irwin's correction, Vergani (2001). In particular, in figure 8 is shown a comparison between the phase maps and the T2 component for three different values of the number of cycles for AISI 410 steel. In the same figure the images were filtered considering a threshold value in order to obtain binary images. The area relative to the phase signal seems does not to change as K_I increases as opposed to the A2 area due to T2 component. In figure 9, the phase signal variation and the maximum value of T2 signal are reported as function of the number of cycles. Also in this case, the phase values seems to change around 20 deg while T2 increases monotonically the number of cycles.
In figures 10 e 11 a comparison between the signals obtained along the crack growth profile is shown for both materials. The distance from a and b represents the plastic area evaluated with the phase signal, a represents also the crack tip position and c the position of the "notional" crack tip. The data for both materials were obtained in correspondence of the same SIF value (K_I=23.6 MPa $m^{1/2}$).

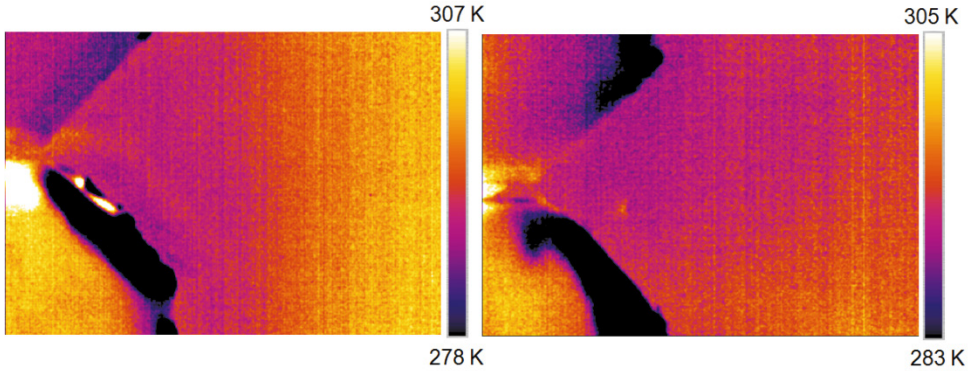

Fig. 3. Temperature images of the AISI steel (left) and CF3M (right) during the test (K_I=23.6 MPa $m^{1/2}$)

For both the materials, A2 area is shifted towards the right with respect to the plastic area obtained with the phase of thermoelastic signal. In particular, A2 area seems placed ahead to the crack "notional" tip and then at the origin of the elastic stress field. The same information provides the phase signal of 2ω component (φ2), in fact, in correspondence of the notional crack tip, the signal decreases abruptly and then changes in sign.

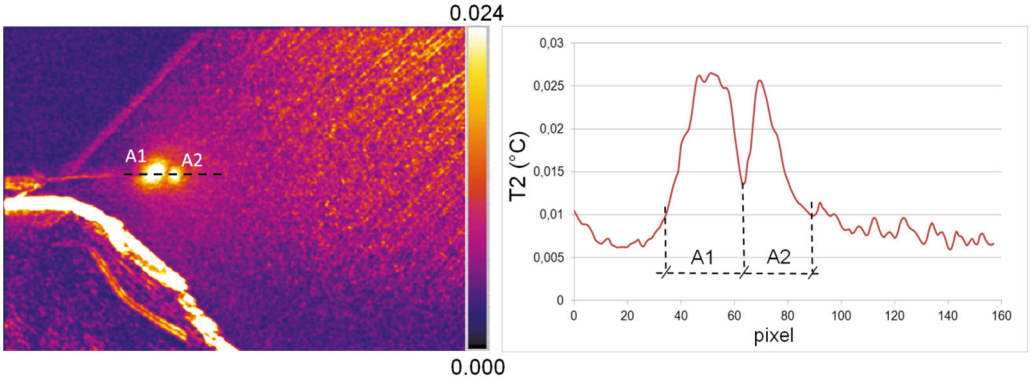

Fig. 4. Amplitude of second Fourier harmonic component (T2) and signal trend along the crack growth direction (AISI 410 steel).

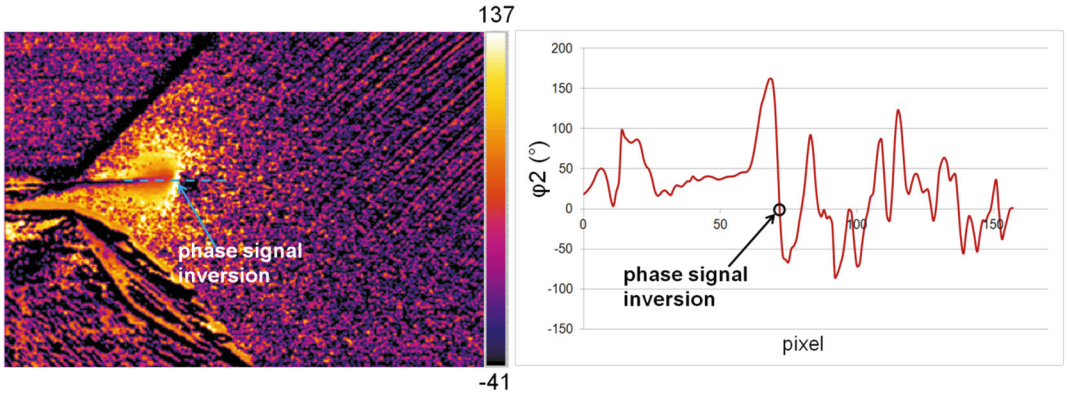

Fig. 5. Phase signal of the second Fourier harmonic component (φ2) and signal trend along the crack growth direction (AISI 410 steel).

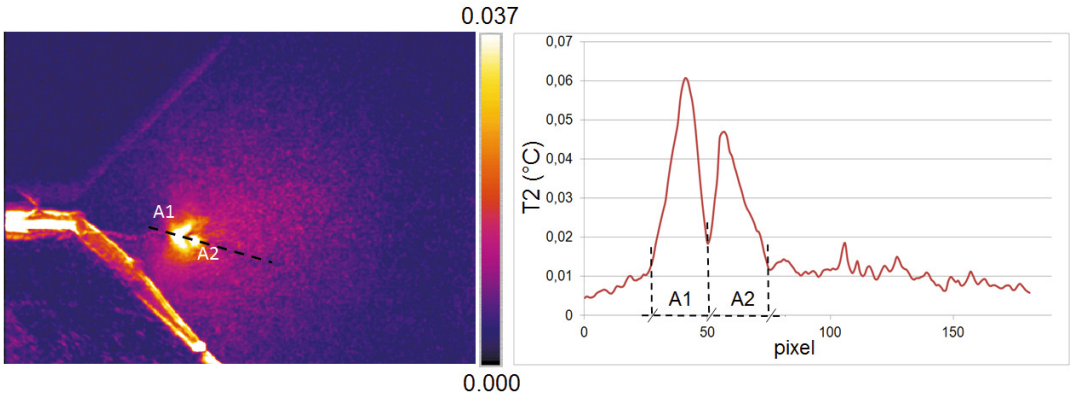

Fig. 6. Amplitude of second Fourier harmonic component (T2) and signal trend along the crack growth direction (CF3M steel).

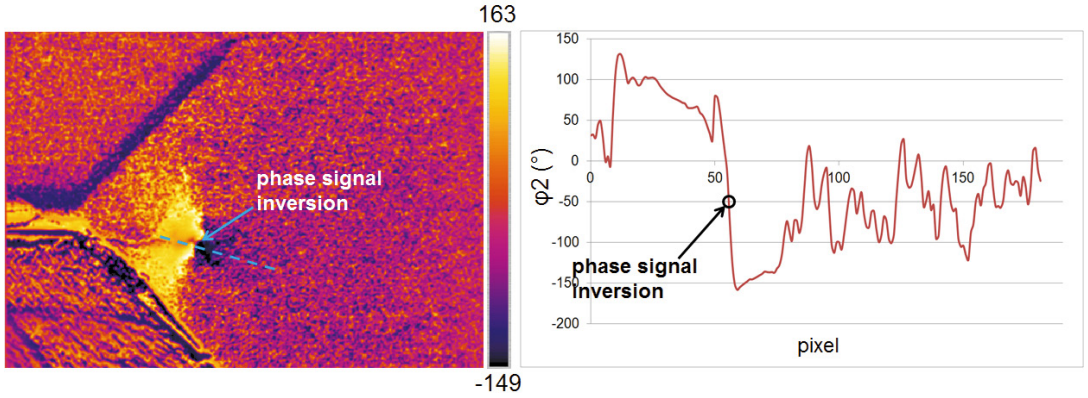

Fig. 7. Phase signal of the second Fourier harmonic component (φ2) and signal trend along the crack growth direction (CF3M steel).

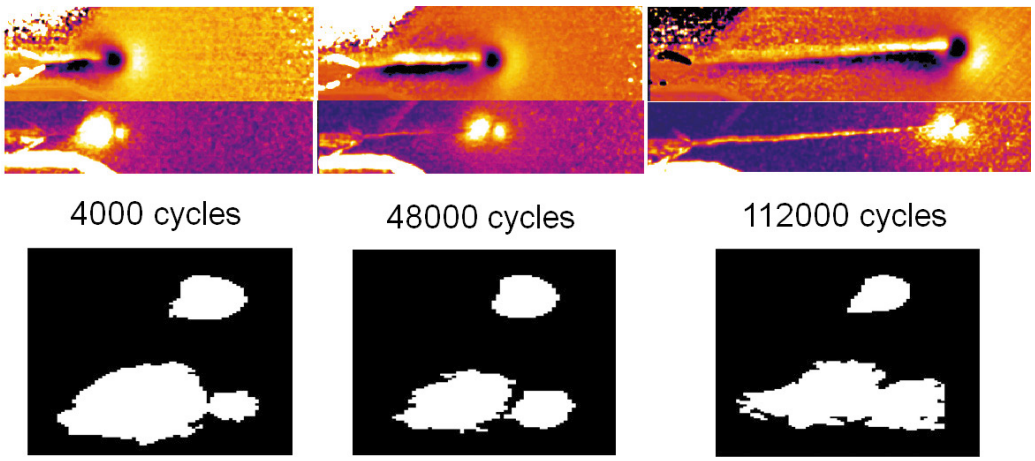

Fig. 8. Fatigue crack growth and binary images of the phase and T2 component at three different values of the crack length.

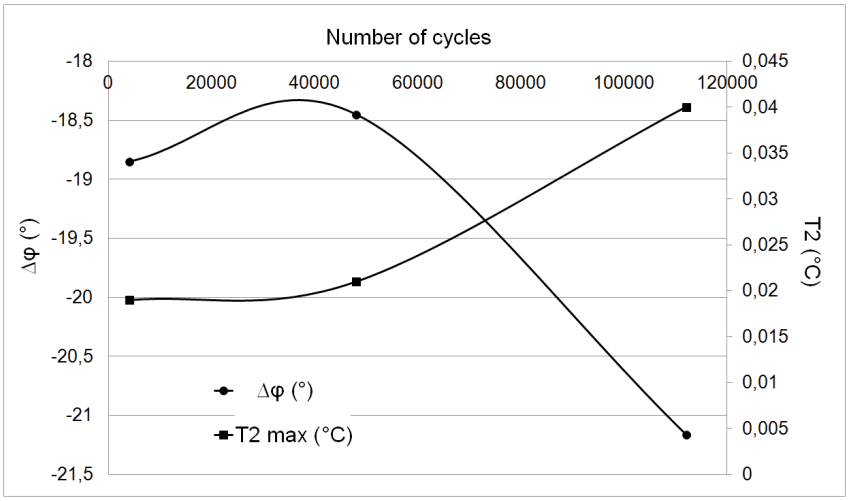

Fig. 9. Phase and T2 max variations with the number of cycles (AISI 410 steel).

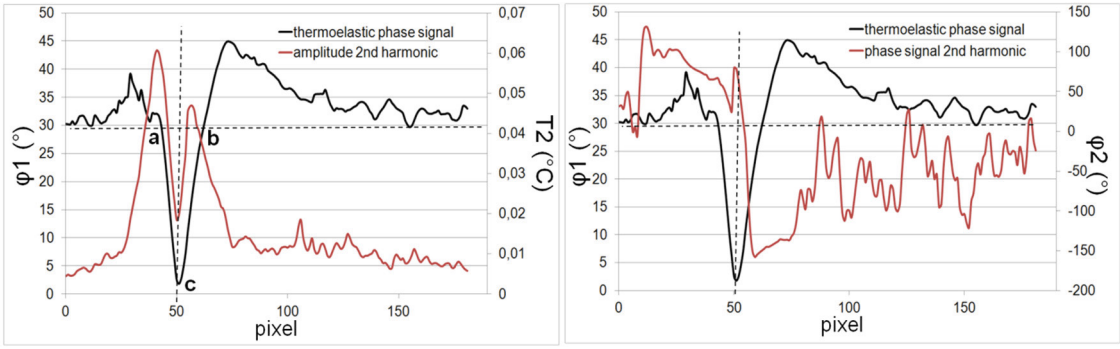

Fig. 10. Comparison between phase signal and amplitude T2 (left) and phase φ2 (right) along a crack growth direction profile (CF3M steel).

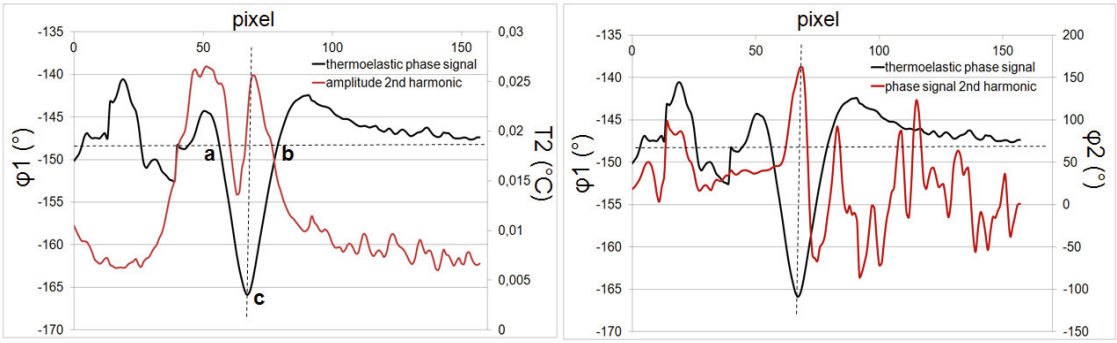

Fig. 11. Comparison between phase signal and amplitude T2 (left) and phase φ2 (right) along a crack growth direction profile (AISI 410 steel).

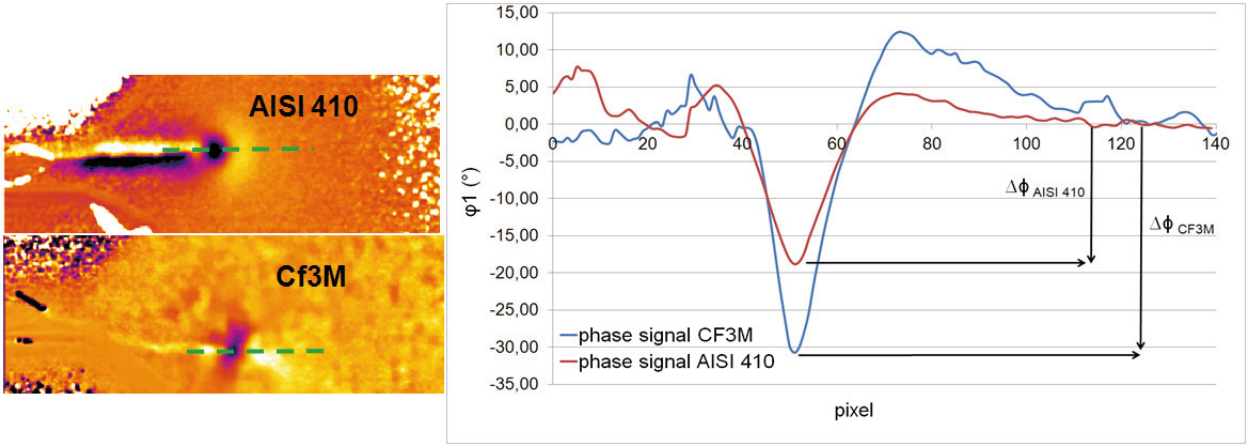

Fig. 12. Comparison between phase signals obtained for both materials in correspondence of K_I=23.6 MPa $m^{1/2}$

Finally, in figure 12, two different values of phase thermoelastic signal were measured for the two kind of steels. Considering the phase signal measured at the point *c* with respect to the phase signal away from the crack in linear elastic conditions (horizontal dotted line) a value of 18.3 degree was obtained for AISI 410 and about 27.9 degree for CF3M. So the thermoelastic phase signal could be used to distinguish between the brittle and the ductile behavior of the material. However, further study are necessary for a better understanding of this parameter.

5. Conclusions

In this work, it was proposed a new thermographic procedure for characterizing the thermal behavior of the crack growth in the material. In particular, the amplitude and phase of the thermal component at the twice the frequency of mechanical loading were studied by means an analysis in the time domain of the temperature signal.

Two stainless steels were tested, the martensitic steel AISI 410 and the austenitic CF3M and the constant-force-amplitude procedure was used on Compact Tension specimens according to Standard. The tests were monitored by using a cooled IR camera and an extension ring in order to obtain a high resolution in the analyzed area.

Thermographic data acquired during the tests were analyzed by adopting a temperature model capable to extract information about the absolute temperature of the specimen, the thermoelastic signal and the second harmonic component of thermographic signal. The attention was focused on this last and in particular on amplitude and phase of the signal. Both the signals provide complementary information with respect to the Thermoelastic Stress Analysis (TSA) usually used for characterizing the fatigue crack of material. In particular, the proposed analysis provides information about the position of the notional crack tip and the heat sources correlated to the plastic deformations and the crack closure.

Acknowledgements

This work is part of a large-scale research project (PON-SMATI) aimed at identifying innovative steels for turbomachinery used in extreme environmental conditions. The authors would like to thank GE oil & gas (Nuovo Pignone S.r.l.) for the support and collaboration provided in the experimental tests.

References

Paris, P., Erdogan F., 1963. A critical analysis of crack propagation laws. Journal of Basic Engineering, Transactions of the American Society of Mechanical Engineers D 85(4), 528-535, DOI: 10.1115/1.3656900.

Ritchie, RO., 1999. Mechanisms of fatigue-crack propagation in ductile and brittle solids. International Journal of Fracture, 100, 55-84.

ASTM E 647-00: Standard Test Method for Measurement of Fatigue Crack Growth Rates, 2004.

Réthore, J., Limodin, N., Buffière, JY., Roux, S., Hild F., 2012. Three-dimensional analysis of fatigue crack propagation using X-Ray tomography, digital volume correlation and extended finite element simulations. Procedia IUTAM 4, 4, 151-159.

Saka, M., Sato, I., Abè, H., 1998. NDE of a 3-D surface crack using magnetic field induced by DC current flow. NDT&E International, 5, 325-329.

Williams, JJ., Yazzie, KE., Padilla, E., Chawla, N., Xiao, X., De Carlo, F., 2013. Understanding fatigue crack growth in aluminium alloys by in situ X-ray synchrotron tomography. International Journal of Fatigue, 57, 79-86.

Kainuma, S., Ahn, JH., Jeong, YS., Takahashi, H., 2015. Evaluation on estimation in characteristics of fatigue crack using micro-encapsulated dye mixing paint. Engineering Failure Analysis, 25, 1-12.

Tanabe, H., Kida, K., Takamatsu, T., Itoh, N., Santos, EC., 2011. Observation of Magnetic Flux Density Distribution around Fatigue Crack and Application to Non-Destructive Evaluation of Stress Intensity Factor. Procedia Engineering, 10, 881-888.

Carrascal, I., Casado, JA., Diego, S., Lacalle, R., Cicero, S., Álvarez, JA., 2014. Determination of the Paris' law constants by means of infrared thermographic techniques. Polymer Testing, 40, 39-46.

Guduru, PR., Zehnder, AT., Rosakis, AJ., Ravichandran, G., 2001. Dynamic full field measurements of crack tip temperatures. Engineering Fracture Mechanics, 68, 1535-1557.

Fedorova, AYU., Bannikov, MV., Plekhov, OA., Plekhova, EV., 2012. Infrared thermography study of the fatigue crack propagation. Frattura ed Integrità Strutturale, 21, 46-54.

Tomlinson, RA., Olden, EJ., 1999. Thermoelasticity for the analysis of crack tip stress fields – a review. Strain, 35, 49-56.

Tomlinson, RA., Patterson, EA., 2011. Examination of Crack Tip Plasticity Using Thermoelastic Stress Analysis. Thermomechanics and Infra-Red Imaging. In: Proceedings of the Society for Experimental Mechanics Series, Volume 7, 123-130.

Diaz, FA., Patterson, EA., Tomlinson, RA., Yates, RA., 2014. Measuring stress intensity factors during fatigue crack growth using thermoelasticity. Fracture of Engineering Materials and Structures, 27(7), 571–584.

Diaz, FA., Patterson, EA., Yates, RA., 2004. Some improvements in the analysis of fatigue cracks using thermoelasticity. International Journal of Fatigue, 26(4), 365–377.

Diaz, FA., Patterson, EA., Yates, RA., 2013. Application of thermoelastic stress analysis for the experimental evaluation of the effective stress intensity factor. Frattura ed Integrità Strutturale, 25, 109-117.

Diaz, FA., Patterson, EA.,Yates, RA., 2005. Differential Thermography Reveals Crack Tip Behaviour?. In: Proc. 2005 SEM Annual Conf. on Exp. App. Mech., Society for Experimental Mechanics, pp. 1413-1419.

Ancona, F., De Finis, R., Palumbo, D., Galietti, U., 2015. Crack growth monitoring in stainless steels by means of TSA technique. Procedia Engineering, 109, 89-97.

Palumbo, D., Ancona, F., De Finis, R., Galietti, U., 2015. Experimental study of the crack growth in stainless steels using thermal methods. Procedia Engineering, 109, 338-346.

Palumbo, D., Galietti, U., 2014. Characterization Of Steel Welded Joints By Infrared Thermographic Methods. Quantitative Infrared Thermography Journal, 11, 42-53.

Galietti, U., Palumbo, D., 2010. Application of thermal methods for characterization of steel welded joints. 14th International Conference on Experimental Mechanics, ICEM 2014; Poitiers; France; 4-9 July 2010. EPJ Web of Conferences, Volume 6, Article number 38012.

Galietti, U., Palumbo, D., De Finis, R., Ancona, F., 2013. Fatigue Damage Evaluation of Martensitic Stainless Steel by Means of Thermal Methods. In: National Conference IGF XXII, 1-3 July, Rome, pp 80-91.

Galietti, U., Palumbo, D., De Finis, R., Ancona, F., 2014. Fatigue limit evaluation of martensitic steels with thermal methods. In: QIRT Conference, 7-11 July, Bordeaux.

Dulieu-Barton, JM., 1999. Introduction to thermoelastic stress analysis. Strain, 35, 35–40.

Pitarresi, G., Patterson, EA., 2003. A review of the general theory of thermoelastic stress analysis. The Journal of Strain Analysis for Engineering Design, 38(5), 405–418.

Wang, WJ., Dulieu-Barton, JM., Li, Q., 2010. Assessment of non-adiabatic behaviour in thermoelastic stress analysis of small scale components. Experimental Mechanics, 50, 449–462.

Harwood, N., Cummings, WM., 1991. Thermoelastic Stress Analysis, Adam Hilger, Bristol Philadelphia and New York.

Palumbo, D., Galietti, U., 2016. Data Correction for Thermoelastic Stress Analysis on Titanium Components. Experimental Mechanics, 56(3), 451-463.

McGuire, MF., 2008. Martensitic Stainless Steels. Stainless Steels for Design Engineers. Asm International. pp. 123-135, ISBN: 978-0-87170-717-8.

Tomei, R., 1981. Criteri di scelta degli acciai inossidabili in funzione degli impieghi. La meccanica italiana. 147.

Rosner, H., Sathish, N., Meyendorf N., 2001. Thermographic characterization of fatigue. Progress in Quantitative Nondestructive Evaluation 20, 1702-1709.

Chrysochoos, A., Wattrisse, B., Muracciole, J-M., El Kaïm Y., 2009. Fields of stored Energy associated with localized necking of steel. Journal of Mechanics and structures, Vol. 4, N.2, Mathematical sciences publishers.

Connesson, N., Maquin, F., Pierron, F., 2011. Experimental Energy Balance During the First Cycles of Cyclically Loaded Specimens Under the Conventional Yield Stress. Experimental Mechanics, 51, 23-45.

Enke, NF., Sandor, BI., 1988. Cyclic plasticity analysis by differential infrared thermography. Proceeding of the VII International Congress on Experimental Mechanics, 830-835.

Sakagami, T., Kubo, S., Tamura, E., Nishimura, T., 2005. Identification of plastic-zone based on double frequency lock-in thermographic temperature measurement. International Conference of Fracture ICF 11.

Krapez, JK., Pacou, D., Gardette, G., 2000. Lock-in Thermography and Fatigue Limit of Metals. Quantitative Infrared Thermography 6, 277-282.

IRTA™ Manual, (2015). Diagnostic Engineering Solutions (DES srl).

Vergani, L., 2001. Meccanica dei materiali, McGraw Hill, Milano, ISBN:88 386 0860-1.